Periodic and quasiperiodic motions of many particles falling in a viscous fluid

Marta Gruca, Marek Bukowicki, and Maria L. Ekiel-Jeżewska*
Institute of Fundamental Technological Research, Polish Academy of Sciences, Pawińskiego 5b, 02-106 Warsaw, Poland
(Received 1 May 2015; published 25 August 2015)

The dynamics of regular clusters of many nontouching particles falling under gravity in a viscous fluid at low Reynolds number are analyzed within the point-particle model. The evolution of two families of particle configurations is determined: two or four regular horizontal polygons (called "rings") centered above or below each other. Two rings fall together and periodically oscillate. Four rings usually separate from each other with chaotic scattering. For hundreds of thousands of initial configurations, a map of the cluster lifetime is evaluated in which the long-lasting clusters are centered around periodic solutions for the relative motions, and they are surrounded by regions of chaotic scattering in a similar way to what was observed by Janosi *et al.* [Phys. Rev. E. **56**, 2858 (1997)] for three particles only. These findings suggest that we should consider the existence of periodic orbits as a possible physical mechanism of the existence of unstable clusters of particles falling under gravity in a viscous fluid.

DOI: 10.1103/PhysRevE.92.023026 PACS number(s): 47.15.G−

I. INTRODUCTION

In various contexts of low-Reynolds-number fluid mechanics, periodic motions have turned out to be essential for the dynamics of particle systems. Jeffery orbits of elongated particles or pairs of spherical particles in shear flow provide a classical example [1]. There has been also a lot of interest in the oscillatory motions of several particles under external force fields. A modern example is a system of several particles kept by external forces inside a toroidal optical trap. Periodic oscillations, hydrodynamic pairing of particles, limit cycles, and transition to chaos have been found in experiments and theoretical models [2–6].

For many decades, periodic settling of a small number of particles under gravity has been studied extensively both experimentally [7–14] and theoretically [15–26], based on the Stokes equations for the fluid flow. A new perspective for the role of such benchmark solutions was provided by Janosi *et al.* [27], who showed that three particles settling under gravity in a viscous fluid in a vertical plane perform chaotic scattering, and they related this behavior to the existence of an unstable periodic solution (which, however, was not directly found). For a wide range of arbitrary random initial configurations, the particles stay together if they are sufficiently close to this periodic solution; the closer they are, the longer they stay together [27]. Later, it was shown that three spheres exhibit a similar chaotic scattering [28], and for spherical particles, the periodic solutions related to chaotic scattering have been explicitly found [29].

It is important to check whether similar behavior can also be observed in the case of clusters made up of a very large number of particles: is chaotic scattering of many particles at nonregular configurations also observed, and is it coupled to periodic oscillations of regular arrays? Is the destabilization pattern of a suspension drop [30,31] related to the existence of periodic solutions for the relative motions of the particles in certain regular configurations, as suggested in Ref. [32]? To address these open challenging problems, the first step is to find and analyze examples of periodic oscillations of a large number of particles settling under gravity in a viscous fluid.

In Ref. [16], periodic oscillations of a cube with the walls parallel and perpendicular to gravity were reported, and it was supposed that other regular polyhedrons may display similar behavior. However, it turned out that the periodic orbits of the cube [16] generalize to another family of periodic oscillations of an arbitrary large (even) number of particles: the particles were arranged in two mirror regular horizontal polygons, one above the other [32]. For a similar geometry of arrays of rods (and other nonspherical particles), centered at vertices of a regular horizontal polygon, periodic solutions have also been found, both experimentally and theoretically [33].

In this paper, we start by generalizing the results of [32], in which periodic solutions were found explicitly for a moderate number of particles centered at vertices of two regular horizontal polygons ("2 rings"). In this work, we explicitly demonstrate that 2 rings made of a very large number of particles indeed fall oscillating periodically. Next, we modify the initial particle positions to obtain a "less regular" configuration, or in other words, we desynchronize the motion of the particles, and we investigate whether periodic solutions can still be found, and if they are related to the existence of clusters with long lifetimes and chaotic scattering of particles in configurations that are close to the periodic orbits.

The modification of the initial conditions is based on the idea of Ref. [32], in which the 2-ring configurations were desynchronized by moving every second particle from each ring to the position it would have after one-fourth of the period. Such a perturbation resulted in the initial configuration of four regular horizontal polygons ("4 rings"), for which long-lasting quasiperiodic relative motions of particles were reported [32]. The question is whether there exist some periodic solutions for an initial configuration close by. Therefore, in this work we investigate in detail the dynamics of 4 rings for a wide range of the initial conditions and different numbers of particles. We evaluate a map of the cluster lifetimes, and we search for periodic solutions and chaotic scattering.

*Author to whom all correspondence should be addressed: mekiel@ippt.pan.pl

II. SYSTEM AND ITS THEORETICAL DESCRIPTION

We investigate the dynamics of regular groups of many point particles settling under identical gravitational forces $\boldsymbol{G}$ in a fluid of viscosity η at a low Reynolds number. The fluid velocity $\boldsymbol{v}$ and pressure p satisfy the Stokes equations (see, e.g., [34]),

$$\eta\nabla^2\boldsymbol{v}(\boldsymbol{r}) - \nabla p(\boldsymbol{r}) = -\sum_{i=1}^{M} \boldsymbol{G}\,\delta(\boldsymbol{r}-\tilde{\boldsymbol{r}}_i), \tag{1}$$

$$\nabla\cdot\boldsymbol{v}(\boldsymbol{r}) = \boldsymbol{0}, \tag{2}$$

where M is the number of particles, $\tilde{\boldsymbol{r}}_i$ denotes the position of the particle with label i, and the z axis is chosen along gravity, with $\boldsymbol{G} = -G\hat{\boldsymbol{z}}$, where $G > 0$ and $\hat{\boldsymbol{z}}$ is the unit vector along the z axis. The equations are written in the laboratory frame of reference.

The fluid velocity $\boldsymbol{v}(\boldsymbol{r})$ and pressure $p(\boldsymbol{r})$ are given by

$$\boldsymbol{v}(\boldsymbol{r}) = \sum_{i=1}^{M} \boldsymbol{T}(\boldsymbol{r}-\tilde{\boldsymbol{r}}_i)\cdot\boldsymbol{G}, \tag{3}$$

$$p(\boldsymbol{r}) = \sum_{i=1}^{M} \boldsymbol{P}(\boldsymbol{r}-\tilde{\boldsymbol{r}}_i)\cdot\boldsymbol{G}, \tag{4}$$

with the Green tensors,

$$\boldsymbol{T}(\boldsymbol{R}) = \frac{1}{8\pi\eta R}\left(\boldsymbol{I} + \frac{\boldsymbol{R}\otimes\boldsymbol{R}}{R^2}\right), \tag{5}$$

$$\boldsymbol{P}(\boldsymbol{R}) = \frac{\boldsymbol{R}}{4\pi R^3}, \tag{6}$$

where $R = |\boldsymbol{R}|$.

The equations of motion of the particles are given by

$$\frac{d\tilde{\boldsymbol{r}}_i}{dt} = \sum_{j\neq i}^{M} \boldsymbol{T}(\tilde{\boldsymbol{r}}_{ij})\cdot\boldsymbol{G} + \mathbf{u}_0, \tag{7}$$

where $\tilde{\boldsymbol{r}}_{ij} = \tilde{\boldsymbol{r}}_i - \tilde{\boldsymbol{r}}_j$, and $\mathbf{u}_0 = \boldsymbol{G}/(6\pi\eta a)$ is the Stokes velocity of the isolated particle. While solving Eqs. (7), it is convenient to follow [32] and choose the inertial frame of reference moving with the velocity $\mathbf{u}_0$. The benefit is that in this frame the dynamics is independent of the additional length scale a. The transformation back to the laboratory frame is straightforward but it is not needed in this work, where we analyze the dynamics in the center-of-mass frame of reference.

From now on, we use dimensionless variables, based on an initial size of the group d as the length unit, and $G/(8\pi\eta d)$ as the velocity unit. Therefore, $8\pi\eta d^2/G$ is the time unit. From now on, $\boldsymbol{r}_i = \tilde{\boldsymbol{r}}_i/d$ denotes the dimensionless position of a particle i.

Initially, the particles are placed at vertexes of K horizontal regular polygons (called "rings") that are separated from each other vertically and centered one above (or below) the other. The diameter d of the top ring is taken as the length unit. The number N of particles in every ring is the same. Therefore, the total number of particles in the system is equal to $M = KN$. Because of the system symmetry, we use the cylindrical coordinate system, in which $\boldsymbol{r}_i$ is represented as $\boldsymbol{r}_i = (\rho_i,\phi_i,z_i)$.

Searching for periodic solutions, we take into account that numerical nonsymmetrical perturbations can destroy periodic unstable solutions after times smaller than the period, as observed in Ref. [32]. Therefore, we symmetrize the dynamics: we force the azimuthal components of the particle velocities to vanish, with $\phi_i = \text{const}(t)$ for $i = 1,\ldots,M$, and the polygons to remain regular for all times. We use the parametrization $i = K(n-1)+k$, with $n = 1,\ldots,N$ and $k = 1,\ldots,K$. Then,

$$\phi_{K(n-1)+k} = \frac{2\pi(n-1)}{N}, \tag{8}$$

and the radial and vertical coordinates of the particles from the same polygon k are the same,

$$\rho_{K(n-1)+k} = \rho_k, \tag{9}$$

$$z_{K(n-1)+k} = z_k \tag{10}$$

for $n = 1,\ldots,N$ and $k = 1,\ldots,K$. The system of $3M$ equations (7) is reduced to the system of $2K$ equations for ρ_l and z_l, with $l = 1,\ldots,K$, which in the frame of reference moving with the velocity $\mathbf{u}_0$ can be explicitly written as

$$\frac{d\rho_l}{dt} = -\sum_{k=1}^{K}\sum_{n=1}^{N} \frac{(z_k-z_l)\left[\rho_k\cos\left(\frac{2\pi(n-1)}{N}\right)-\rho_l\right]}{R_{lkn}^3}, \tag{11}$$

$$\frac{dz_l}{dt} = -\sum_{k=1}^{K}\sum_{n=1}^{N}\left(\frac{1}{R_{lkn}} + \frac{(z_k-z_l)^2}{R_{lkn}^3}\right), \tag{12}$$

$$R_{kln}^2 = (z_k-z_l)^2 + \rho_l^2 + \rho_k^2 - 2\rho_l\rho_k\cos\left(\frac{2\pi(n-1)}{N}\right). \tag{13}$$

The numerical integration of Eqs. (11)–(13) is based on two methods: the fourth-order adaptive Runge-Kutta method for nonstiff problems, and the backward differentiation formula (BDF) for stiff problems. We solve a system of ordinary differential equations using lsoda from the FORTRAN library odepack. Initially we start with a nonstiff solver. Depending on the number of time steps and the accuracy, the solver switches between methods that are appropriate for the stiff or nonstiff problem. This procedure is a standard and commonly used method for solving differential equations. This solver is sufficiently stable [35]. The numerical calculations were performed with double precision, and the error per each time step is not greater than 10^{-12}.

We are interested in the relative motion of the particles; therefore, we will trace their positions in the center-of-mass frame of reference, located at the symmetry axis, $\boldsymbol{r}_{\text{CM}} = (0,0,z_{\text{CM}})$. In this frame, ρ_i and ϕ_i are the same as in the laboratory frame, and particle vertical coordinates are $Z_i = z_i - z_{\text{CM}}$.

We perform simulations for two families of the systems: with two and four rings. The specific initial configurations and their evolution will be discussed in the next sections.

III. DYNAMICS OF 2 RINGS

We first consider a system of $M = 2N$ particles that are grouped in two horizontal rings, each containing N equally spaced particles. Initially, the rings are identical and placed

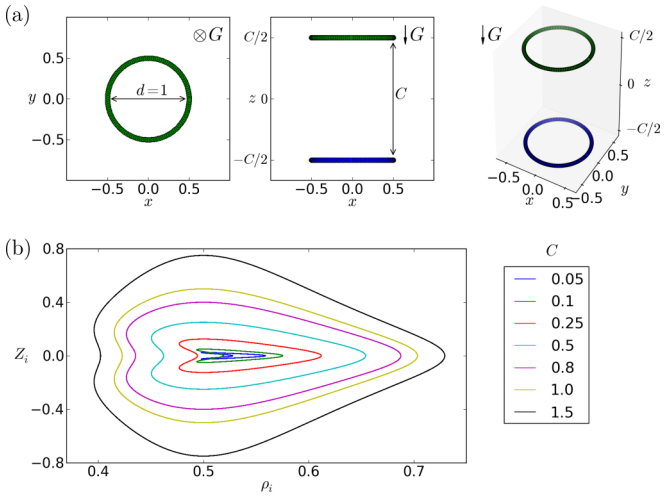

FIG. 1. (Color online) The system of M particles that form 2 rings. (a) $M = 256$. The initial configuration as in Eq. (15). (b) $M = 20\,000$. In the center-of-mass frame, the trajectory of each particle has the same shape (not drawn to scale). Different shapes correspond to the indicated values of C.

one exactly above the other. The diameter of each ring is equal to $d = 1$ and the initial distance C between the rings is a parameter in our simulations, as shown in Fig. 1(a). The initial positions $\boldsymbol{r}_i = (\rho_i, \phi_i, z_i)$ of the particles $i = 1, \ldots, M$ are

$$\boldsymbol{r}_{2n-1} = \left(\frac{1}{2}, \frac{2\pi(n-1)}{N}, \frac{C}{2}\right), \tag{14}$$

$$\boldsymbol{r}_{2n} = \left(\frac{1}{2}, \frac{2\pi(n-1)}{N}, -\frac{C}{2}\right), \tag{15}$$

with $n = 1, \ldots, N$. We conducted around 100 simulations for $M = 256$ and 20 000 particles and different initial values of $C \in [0.05, 2.5]$. For these values of the parameters, we observe the periodic motion of the particles during the whole simulation time $t = 5000$ (which corresponds to 300–2700 periods); see our movie 1 in [36].

In the center-of-mass frame, two particles with the same angular coordinates move along the same trajectory. Its shape is the same for all the pairs, and it depends on C as shown in Fig. 1(b) for $M = 20\,000$. We found similar families of shapes for $M = 256$, analogical to those reported by [32] for $M = 16$, and resembling periodic solutions for rigid rods, discussed by [33] and [37].

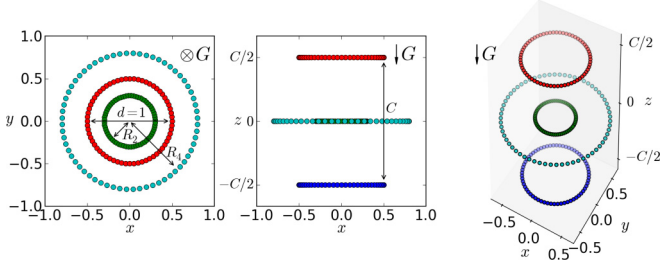

FIG. 2. (Color online) Initially, M particles form 4 rings, as specified in Eq. (19). Here, $M = 256$.

IV. DYNAMICS OF 4 RINGS

A. Initial configurations

In the second system, $M = 4N$ particles are grouped in four horizontal rings, each consisting of N particles. Initially, the rings labeled 1 and 3 are placed at $z = C/2$ and $-C/2$, respectively, and the rings labeled 2 and 4 are placed at $z = 0$, as shown in Fig. 2(a). The radii of the rings 1, 3, 2, and 4 are equal to $1/2$, $1/2$, R_2, and R_4, respectively, with $R_4 > R_2$. The angular coordinates of the particles from ring 1 and ring 3 are the same. The other rings are rotated by π/N around the symmetry axis. Summarizing, the initial cylindrical coordinates of the particles are

$$\boldsymbol{r}_{4n-3} = \left(\frac{1}{2}, \frac{2\pi(n-1)}{N}, \frac{C}{2}\right), \tag{16}$$

$$\boldsymbol{r}_{4n-2} = \left(R_2, \frac{2\pi(n-\frac{1}{2})}{N}, 0\right), \tag{17}$$

$$\boldsymbol{r}_{4n-1} = \left(\frac{1}{2}, \frac{2\pi(n-1)}{N}, -\frac{C}{2}\right), \tag{18}$$

$$\boldsymbol{r}_{4n} = \left(R_4, \frac{2\pi(n-\frac{1}{2})}{N}, 0\right), \tag{19}$$

where $n = 1, \ldots, N$, and R_2 and R_4 are the parameters of the simulation.

We performed around 400 000 simulations for clusters made of different numbers of particles $M = 64, 256, 1024$ at the initial configurations specified by Eqs. (17)–(19), with $C \in [0.05, 2.5]$, and a wide range of R_2 and R_4. In Secs. IV B–IV E we will analyze how the dynamics depends on R_2 and R_4 for $M = 256$ and $C = 1.5$. Then, in Sec. IV F, we will argue that these results are generic also for the other values of M and C.

B. Basic features of the dynamics

The dynamics of four rings of particles is more complex than the dynamics of two rings. Although the general pattern of oscillations combined with settling is maintained, in the case of four rings the motion in general is not periodic and we observe destabilization and decay of the system, as in movie 2; see [36]. The majority of initial conditions lead to the system decay during the first 1000 units of the simulation time, which corresponds to about 100 oscillations.

If the group breaks up, usually one ring is left behind the other three or one ring falls faster than the rest of the group; we call this a "3+1" type of decay. If the system separates into two pairs of rings, we denote it as a "2+2" type of decay. We observe also a "2+1+1" type of decay when two rings oscillate together and the others are separated. Examples of each decay type are presented in Figs. 3(a)–3(c) and movies 3 a-c in [36].

For certain initial configurations, the particles perform quasiperiodic motion over a very long time. It has been checked that for several thousand values of R_2 and R_4, the cluster lifetime exceeds 100 000. A typical shape of the corresponding trajectory $Z_i(\rho_i)$ is shown in Fig. 3(d) and movie 3 d; see [36]. These findings may indicate that for certain values of R_2 and

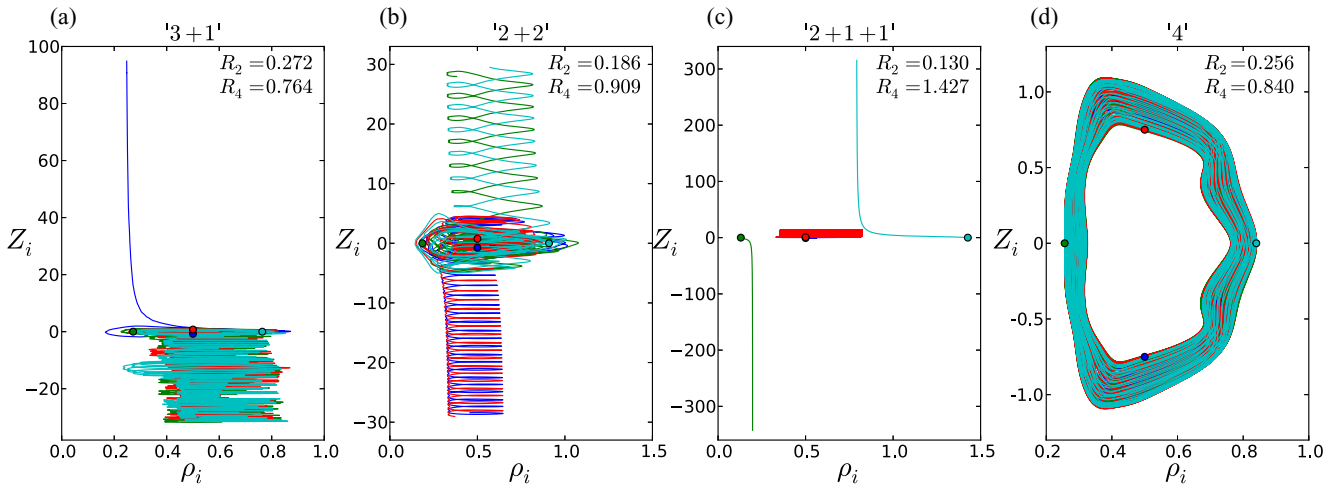

FIG. 3. (Color online) Evolution of $M = 256$ particles that form 4 rings with $C = 1.5$ and R_2,R_4 as indicated. Trajectories of four particles (each from a different ring) in the center-of-mass reference frame until time $t = 500$. The initial positions are marked by dots. (a) "3+1" type of decay. One of the rings separates from the cluster. (b) "2+2" type of decay. The group breaks up into two pairs of oscillating rings—one of them falls faster than the other. (c) "2+1+1" type of decay. The cluster breaks up into one pair of oscillating rings and two single rings. (d) "4": lack of decay. All rings oscillate.

R_4, periodic solutions exist, and they will be searched for later in this paper.

We would like to remind the reader that all simulations are performed for symmetrized configurations, and the particles by definition do not change the vertical planes to which they belong, as described in Sec. II. The symmetrization is done on purpose to find periodic solutions and to ensure that the system will not break up because of nonsymmetrical numerical perturbations before a period is completed.

C. Decay of the cluster

To describe the system dynamics, it is crucial to define the event of the cluster decay and its time, denoted as τ. The intrinsic property of a cluster of particles settling under gravity is the existence of periodic relative motions, which may be used as an indicator of whether the particles move together and interact with each other. For this reason, we introduce a criterion of a cluster decay based on the presence or absence of oscillations between pairs of particles. In particular, oscillations of particles i and j that belong to the same group imply that the difference in their z coordinates, $\Delta z_{ij} = z_i - z_j$, oscillates around zero. We recognize that the particles i,j interact and stay together if Δz_{ij} has repeating roots.

Therefore, we use the following definition of the cluster decay. For each pair of particles i,j we calculate the difference Δz_{ij} of their z coordinates as a function of time. If for any l,m the time interval between two consecutive roots, t_A and $t_B > t_A$, of Δz_{lm} exceeds 1000, we classify it as the cluster decay and denote $\min_{l,m} t_A$ as the cluster lifetime τ.

This criterion of decay works well, in contrast to attempts based on measuring only the relative vertical distances between rings, because it is common that rings approach each other again, even if they were separated by a very long vertical distance, as observed in [28] for systems of three particles.

To define the type of cluster decay, we apply the following procedure: we count the number of roots of Δz_{ij} in the time interval $[\tau,\min(\tau + 1000,T)]$ for each pair of particles ij. If the number of roots is smaller than the length of the time interval divided by 200 (for the interval $[\tau,\tau + 1000]$ it is equal to 5), we define that the particles i,j interact with each other. Otherwise, we denote them as separated. The number L of interacting pairs indicates the type of decay. $L = 3$ corresponds to the "3+1" type of decay, $L = 2$ to the "2+2" type of decay, $L = 1$ to the "2+1+1" type of decay, and $L = 0$ to "1+1+1+1." For $L = 6$ there is no decay (type "4").

Now, the main question is how the lifetime depends on the initial conditions. The results are presented in Fig. 4 as a map in space of the parameters R_2 and R_4, with colors indicating the logarithm of the cluster lifetime. Values of R_2 and R_4 that lead to long-living clusters form a few compact regions, around which only isolated configurations with long lifetimes can be found. Deterministic regions are visible when R_2 is small enough, or R_4 is large enough, and the cluster splits up immediately without oscillations. In the first case, the settling velocity of a very small ring 2 is much larger than the velocities of the other rings, while in the second case, the settling velocity of a very large ring 4 is much smaller than the velocities of the other rings.

The essential property of the map shown in Fig. 4 is that for a wide range of R_2 and R_4, the cluster lifetime is very sensitive to the initial conditions. Around the regions of long-living clusters (with very sharp edges), we find a variability of the cluster lifetime by orders of magnitude. This property is also well visible in Fig. 5 at the cross sections of the map, plotted on a linear scale. This behavior is similar to the chaotic scattering reported in [27] for three point particles sedimenting in a vertical plane.

In Fig. 6, we show the type of cluster decay and labels of the particles that interact with each other at the decay time τ, depending on R_2 and R_4. Sensitivity to initial conditions is clearly visible in most of the map areas, except for a few deterministic regions corresponding to a very long or a very short lifetime. The last ones can be easily understood by comparing the ring diameters, and taking into account that the smaller the ring, the larger is its velocity.

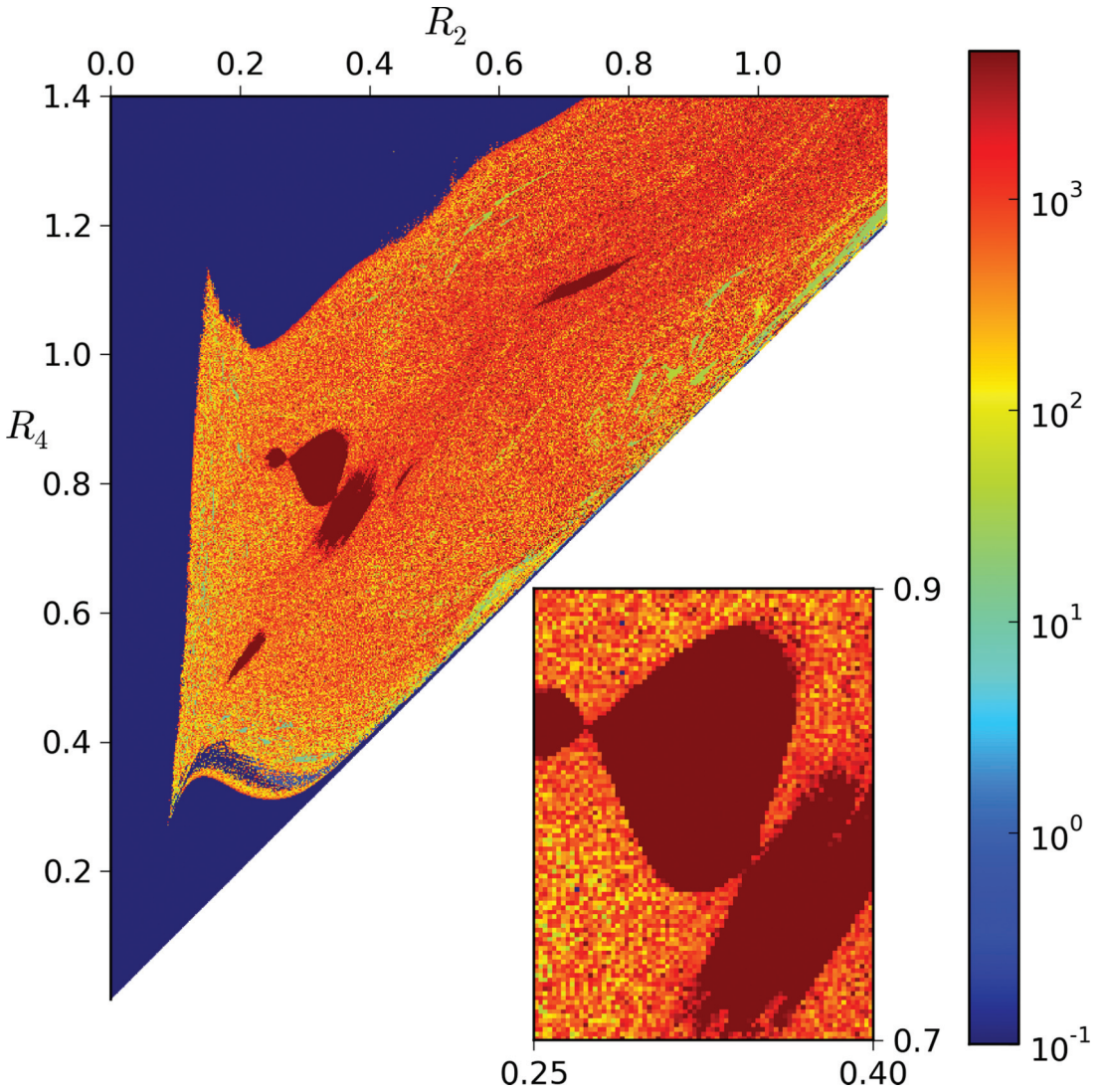

FIG. 4. (Color) The cluster lifetime for around 420 000 initial configurations with $C = 1.5$ and different values of R_2 and R_4 (drawn to scale). The darkest red corresponds to the cluster lifetime larger than the simulation time $t = 5000$. The resolution of the map is 0.002×0.002 and $M = 256$.

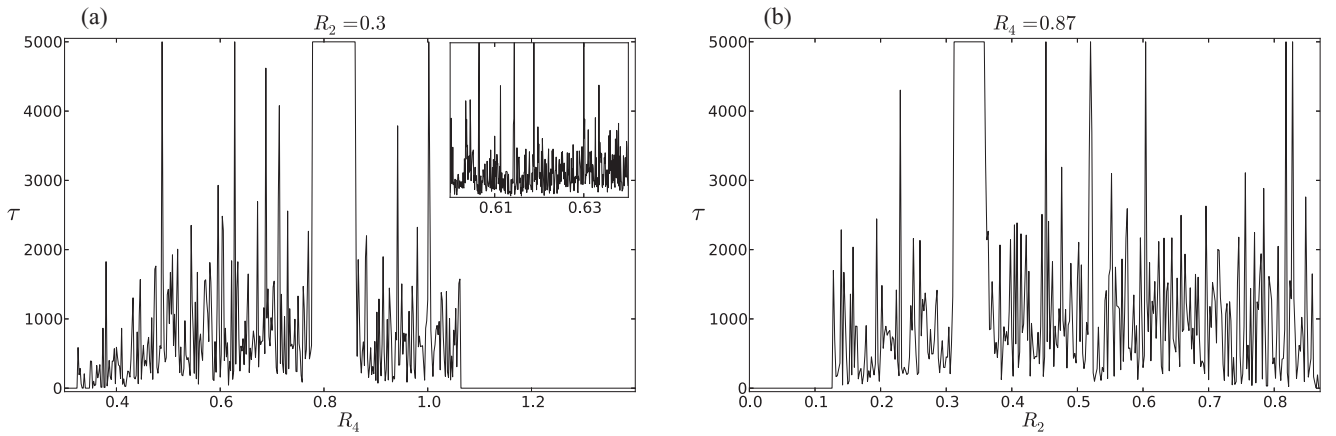

FIG. 5. Cross sections (now in linear scale) through the map of the cluster lifetime from Fig. 4: (a) $R_2 = 0.3$, (b) $R_4 = 0.87$. Sensitivity to initial conditions is clearly visible. Inset: Scaling down the resolution of R_2 and R_4 from 0.002 to 10^{-4}, a self-similar structure is found.

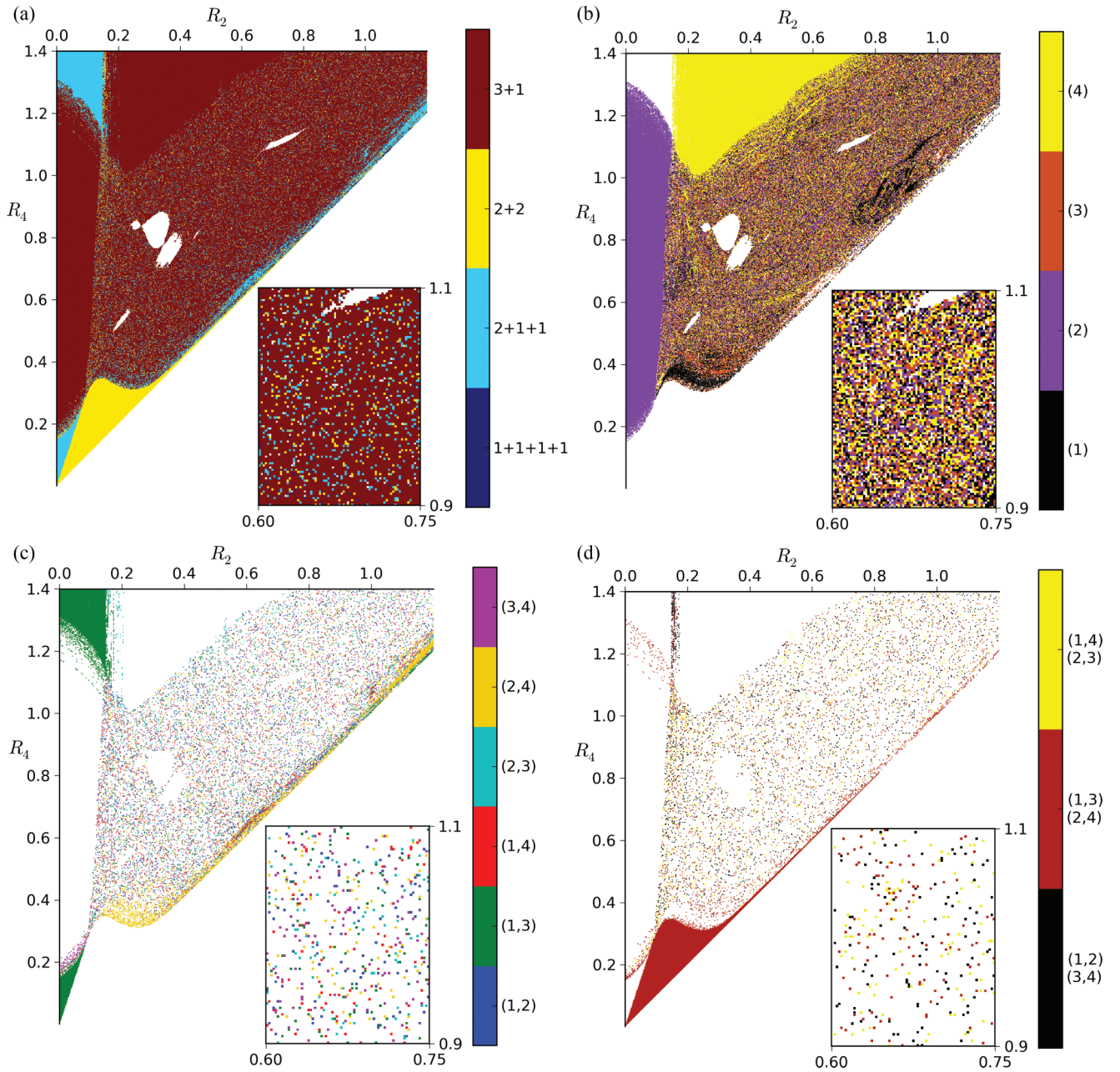

FIG. 6. (Color) Sensitivity of patterns of the cluster decay to the initial parameters R_2 and R_4, for $C = 1.5$ and $M = 256$. White means no decay. (a) The types of decay: into "3+1," "2+2," "2+1+1," or "1+1+1+1" rings (see Sec. IV C for the exact definitions). (b) "3+1" type of decay: the color indicates the label of the ring that separates from the others at time τ. (c) "2+1+1" type of decay: the colors indicate the interacting pair of the rings at time τ. (d) '2+2" type of decay: the colors indicate which rings form interacting pairs at time τ.

D. Clusters with long lifetimes and quasiperiodic solutions

We have found that the long lifespan of the cluster and the quasiperiodic trajectories of the particles are observed for the system with initial configurations grouped in a few regions (see Fig. 4). We will now investigate trajectories from each of the specific long-lifetime regions, and search for periodic solutions.

Toward that end, we apply the dynamic time warping (DTW) method, described, e.g., in [38] and [39]. For each particle i, we define its reference trajectory $Z_i^r(\rho_i)$ for times $t_1 \leqslant t \leqslant t_3$, where t_k, $k = 1,2,3$, are the first, second, and third time instants when $Z_i(t_k) = 0$. Then, for $t_3 \leqslant t \leqslant 5000$, we calculate the Euclidean distance $d_i(t)$ between the particle position $(Z_i(t), \rho_i(t))$ and its reference trajectory. We define the average deviation Δ of the trajectories as the average of $d_i(t)$ over all the particles i and all times t.

In Fig. 4, we surround three main long-lifetime islands in R_2–R_4 space by rectangular boxes of a fixed resolution, and we evaluate for each pixel the average deviation Δ of the trajectories. The results are shown in Fig. 7. For each

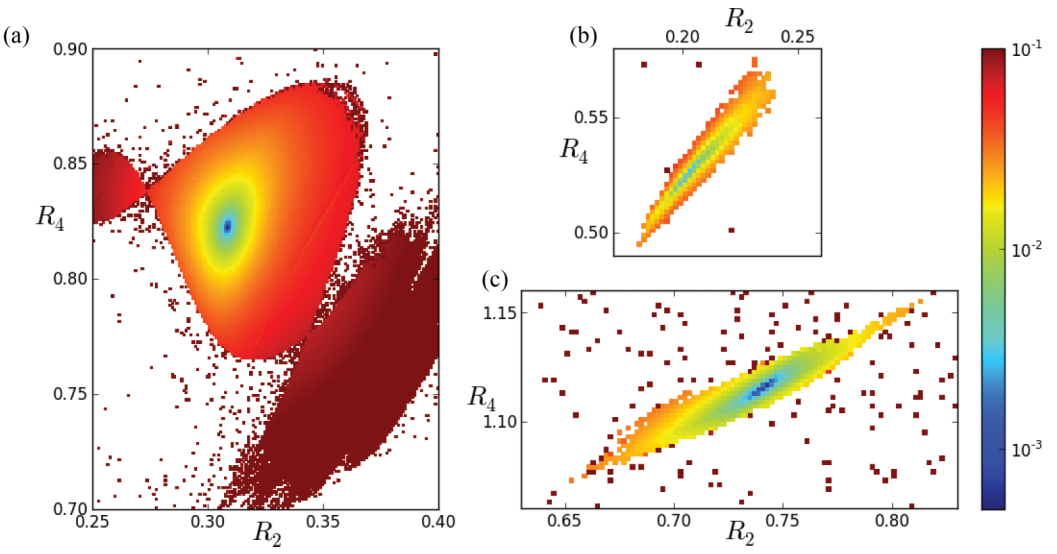

FIG. 7. (Color) The average deviation Δ of particle trajectories for clusters with lifetimes $\tau \geqslant 5000$, $C = 1.5$, and $M = 256$. Resolution: (a) 0.001×0.001; (b) and (c) 0.002×0.002. The minima in (a), (b), and (c) correspond to the solutions presented in Figs. 8(a), 8(b), and 8(c), respectively.

of the three boxes, there exists the smallest deviation $\Delta_{\min}$, corresponding to a very thin trajectory. For example, in Fig. 7(a), $\Delta_{\min} = 3 \times 10^{-4}$ is 300 times smaller than the deviation of the quasiperiodic trajectories shown in Fig. 3(d).

E. Three periodic solutions

The minima visible in Figs. 7(a), 7(b), and 7(c) correspond to three periodic trajectories in the center-of-mass frame of the cluster, shown in Figs. 8(a), 8(b), and 8(c), respectively.

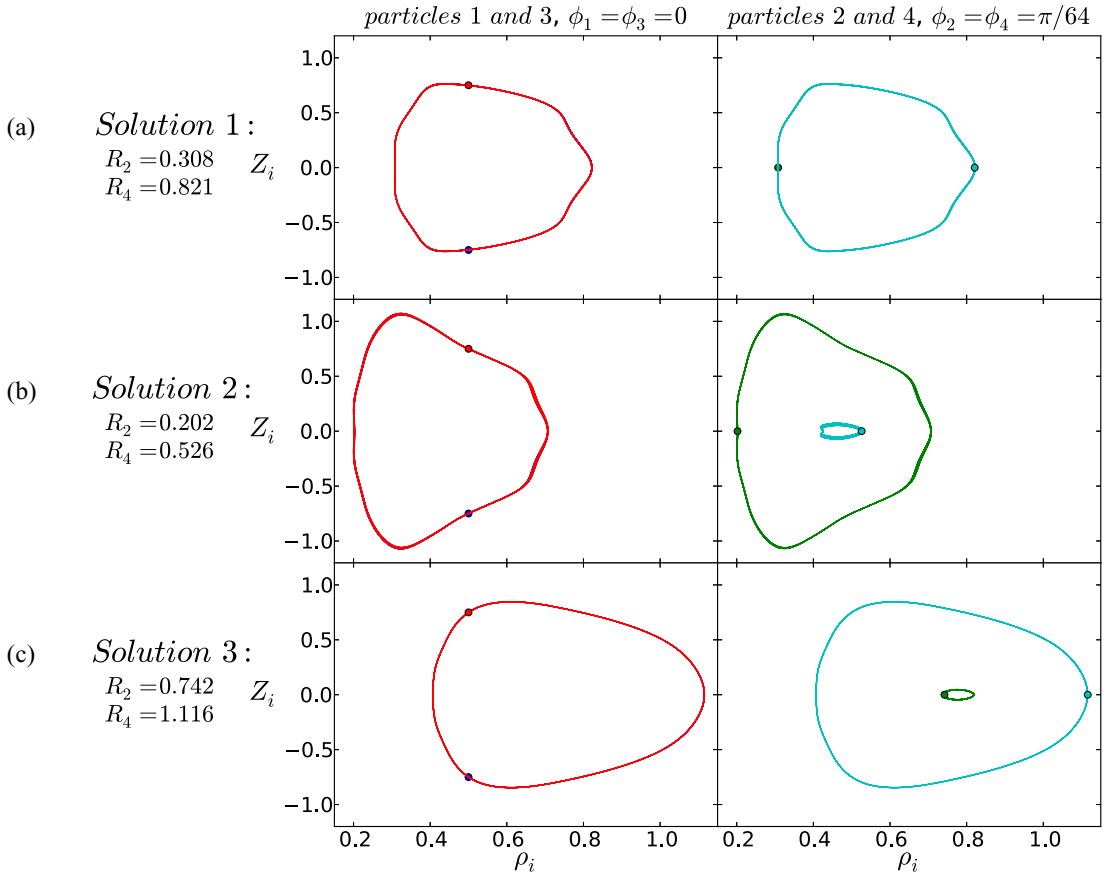

FIG. 8. (Color online) Periodic trajectories of four particles (each from a different ring) in the center-of-mass frame of a cluster with $M = 256$ particles. Dots: the initial particle positions, with $C = 1.5$. Solutions in (a)–(c) correspond to the minima of Δ in Figs. 7(a)–7(c), respectively.

We remind the reader that due to the symmetrization of the dynamics, each particle from ring i has the same coordinates $Z_i(t)$ and $\rho_i(t)$. Therefore, it is sufficient to display $Z_i(\rho_i)$ for particles $i = 1,2,3,4$, each from a different ring i, with particles 1,3 moving in a vertical plane $\phi = 0$ and particles 2,4 moving in another vertical plane $\phi = 4\pi/M$. Here, $M = 256$ and $C = 1.5$.

The periodic solutions have the following properties.

Solution 1, shown in Fig. 8(a) and movie 8 a in [36], is located in the middle of the biggest of the long-lifetime regions from Fig. 4, and at the minimum of the deviation Δ of the trajectories in Fig. 7(a). All four particles move along the same trajectory $Z_i(\rho_i)$, shifted in phase by $T/4$, with the period $T = 11.7$.

Solution 2, shown in Fig. 8(b) and movie 8 b in [36], is located in the middle of a small long-lifetime region from Fig. 4, and at the minimum of the deviation Δ of the trajectories in Fig. 7(b). It corresponds to the initial radius R_2 of ring 2 much less than the initial radius of rings 1 and 3, $R_1 = R_3 = 0.5$, and with $R_4 \gtrsim 0.5$. The central particle 4 has its own tiny trajectory and is circulated by the other three, which move along a larger trajectory with the period $T = 10.7$, shifted in phase by $T/3$ with respect to each other. The period of particle 4 is equal to $T/3$.

Solution 3, shown in Fig. 8(c) and movie 8 c in [36], is located in the middle of the other small long-lifetime region from Fig. 4, and at the minimum of the deviation Δ of the trajectories in Fig. 7(c). The corresponding initial configuration satisfies the relations, $R_2, R_4 > R_1 = R_3 = 0.5$. Now particle 2 is the central one, and the motion is qualitatively similar to solution 2, with the interchange of particles 2 and 4. In addition, the rings are much wider, which leads to a larger period, $T = 15.6$, because larger rings move slower.

F. Two families of periodic solutions

Periodic oscillations have been found for many values of C. In Fig. 9 we show how the shape of the periodic trajectory of type 1 depends on C. Periodic solutions 1, 2, and 3 for $C = 2$ are shown in Fig. 10. These examples illustrate that the basic properties of the periodic solutions, described in the previous section and shown in Fig. 8, are generic for a wide range of values of C.

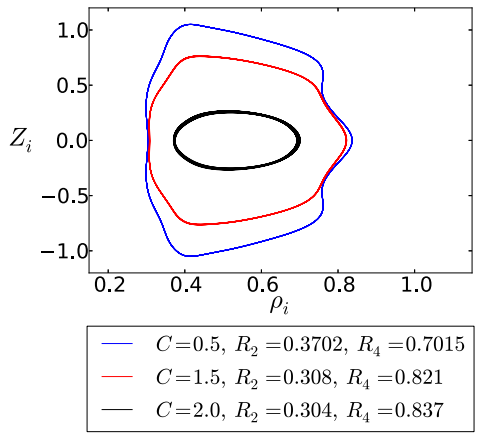

FIG. 9. (Color online) Periodic solutions of type 1 for different values of C and $M = 256$.

Initially, two particles are at the same horizontal plane, and the other two particles are exactly one above the other. Movies 8 b,c in [36] illustrate that for each periodic solution 2 or 3, such a configuration appears again at $T/6$, but with *different* values of C, R_2, and R_4, which correspond to solutions 3 or 2, respectively. This configuration can be treated as another initial condition for the same periodic solution. Therefore, assuming that there exist periodic solutions for all sufficiently large values of C, we predict the existence of twin solutions 2 and 3 for each value of C that is large enough. The dynamics of 4 rings made of other numbers $M = 64$ and 1024 of the particles has also been evaluated, and similar families of periodic solutions have been found.

V. DISCUSSION AND CONCLUDING REMARKS

In this work, we searched for the periodic relative motions of many particles that form regular clusters with aspect ratios of the order of 1. We generalized in this way the previous solutions found in Ref. [32] for a smaller number of particles. In Ref. [32], the systems of 2 rings were shown to destabilize. Therefore, to determine accurately periodic motions, in this paper we solved the symmetrized dynamics, given in Eqs. (11)–(13). Although we have not analyzed here the nonsymmetric perturbations, it is known from Ref. [32] that such perturbations destabilize the system after times that are large enough to observe the existence of periodic solutions and determine the cluster lifetimes (e.g., for 64 particles, periodic motions destabilize at times t not shorter than half of the period, $T/2$, while even the motion during $T/4$ would be sufficient to deduce the existence of unstable periodic solutions).

A similar behavior was observed experimentally in Ref. [14] for three close particles sedimenting approximately in a vertical plane. Typically, periodic motions have been observed during times comparable to one-sixth of the period, $T/6$. Due to the symmetries of the motion, this is sufficient to demonstrate the existence of unstable periodic orbits. Moreover, in these experiments, the same type of periodic orbit was reached again after the destabilization, and this pattern of approaching and leaving the periodic orbit was repeated several times. Summarizing, examples of unstable periodic motions can be easily observed in experiments, and sometimes unstable periodic motions form a generic feature of the dynamics.

In this work, we found a surprisingly large number of periodic solutions. For a cluster made of 2 rings, they were observed for all the investigated shapes (parametrized by moderate values of the initial aspect ratio C), and for particle numbers N even as large as 20 000.

It has been interesting to modify the initial 2-ring configuration, with particles arranged in four rings, and in this way desynchronized. It turned out that clusters made of four rings usually break up, and their lifetime and type of decay are generally sensitive to initial conditions. In the 2D space of initial parameters, the deterministic area surrounds the chaotic region. The last one contains islands of quasiperiodic oscillations that do not destabilize during extremely long

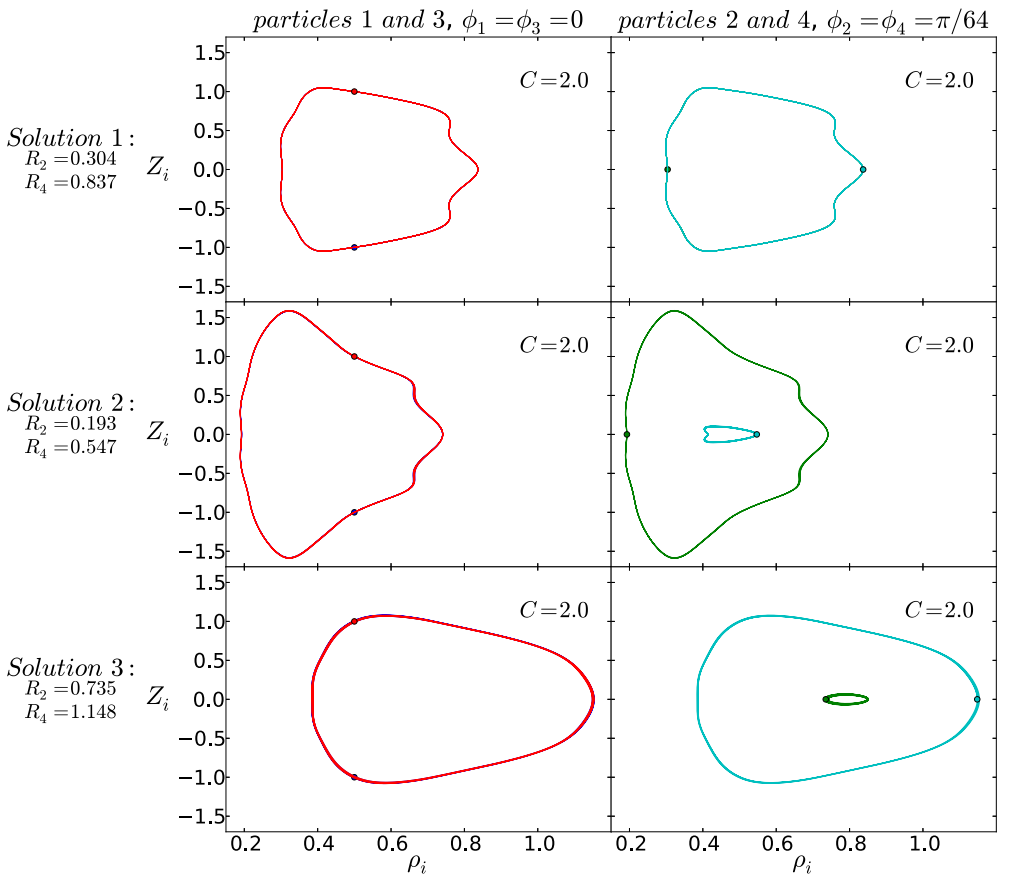

FIG. 10. (Color online) Periodic trajectories of four particles (each from a different ring) in the center-of-mass frame of a cluster with $M = 256$ particles. Dots: the initial particle positions. Here, $C = 2.0$ (compare with Fig. 8, where $C = 1.5$).

simulation times. At the centers of these islands, three different periodic solutions exist, parametrized by the initial cluster height and the number of particles.

The results provide a new perspective for the physical mechanism of the decay of particle clusters sedimenting in a viscous fluid, typically with a very wide range of lifetimes.

ACKNOWLEDGMENTS

This work was supported in part by the Polish National Science Centre, Grant No. 2011/01/B/ST3/05691. We benefited from scientific activities of the COST Action MP1305.

APPENDIX: PERIODIC TRAJECTORIES FOR A DIFFERENT VALUE OF THE PARAMETER *C*

In this appendix, we illustrate that Fig. 8 (with $C = 1.5$) provides a generic example of two families of periodic solutions: solution 1 corresponds to the first family and solutions 2 and 3 to the second family, as discussed in Sec. IV F. This type of structure of the periodic solutions has been observed for many values of the parameter C, which determines the initial geometry of the upper and lower rings. In Fig. 10, we show another example: the periodic orbits for $C = 2$ (compare with Fig. 8).

[1] G. Jeffery, Proc. R. Soc. **102**, 161 (1922).
[2] M. Reichert and H. Stark, J. Phys.: Condens. Matter **16**, S4085 (1991).
[3] C. Lutz, M. Reichert, H. Stark, and C. Bechinger, Europhys. Lett. **74**, 719 (2006).
[4] Y. Roichman, D. G. Grier, and G. Zaslavsky, Phys. Rev. E **75**, 020401(R) (2007).
[5] Y. Sokolov, D. Frydel, D. G. Grier, H. Diamant, and Y. Roichman, Phys. Rev. Lett. **107**, 158302 (2011).
[6] Y. Sassa, S. Shibata, Y. Iwashita, and Y. Kimura, Phys. Rev. E **85**, 061402 (2012).
[7] K. O. L. F. Jayaweera, B. J. Mason, and H. W. Slack, J. Fluid Mech. **20**, 121 (1964).
[8] B. H. Kaye, Ph.D. thesis, London Univ. (1961).
[9] B. Koglin, Chem. Ing. Tech. **44**, 515 (1972).
[10] B. Koglin, Habilitation thesis, Karlsruhe Univ. (1973).
[11] B. Koglin and A. Al-Taweel, in *Harold Haywood Memorial Symposium* (Loughborough University of Technology, Loughborough, UK, 1973).

[12] B. Koglin, A. Al-Taweel, and N. Ahmad, Chem. Ing. Tech. **48**, 557 (1976).
[13] S. Alabrudziński, M. L. Ekiel-Jeżewska, D. Chehata-Gómez, and T. A. Kowalewski, Phys. Fluids **21**, 73302 (2009).
[14] J. Nowakowski and M. L. Ekiel-Jeżewska, Gallery of Fluid Motion, 67th Annual Meeting of the APS Division of Fluid Dynamics.
[15] L. M. Hocking, J. Fluid Mech. **20**, 129 (1963).
[16] L. Durlofsky and J. F. Brady, J. Fluid Mech. **180**, 21 (1987).
[17] R. E. Caflisch, C. Lim, J. H. C. Luke, and A. S. Sangani, Phys. Fluids **31**, 3175 (1988).
[18] M. T. Kamel and E. M. Tory, Powder Technol. **63**, 187 (1990).
[19] E. M. Tory, M. T. Kamel, and C. B. Tory, Powder Technol. **67**, 71 (1991).
[20] M. Golubitsky, M. Krupa, and Ch. Lim, SIAM J. Appl. Math. **51**, 1 (1991).
[21] E. M. Tory and M. T. Kamel, Powder Technol. **73**, 95 (1992).
[22] Ch. C. Lim and I. H. McMomb, J. Differ. Eqs. **121**, 2 (1995).
[23] I. K. Snook, K. M. Briggs, and E. R. Smith, Physica A **240**, 547 (1997).
[24] M. L. Ekiel-Jeżewska, T. Gubiec, and P. Szymczak, Phys. Fluids **20**, 63102 (2008).
[25] M. Bargieł, M. T. Kamel, and E. M. Tory, Powder Technol. **214**, 14 (2011).
[26] M. Bargieł and E. M. Tory, Powder Technol. **264**, 519 (2014).
[27] I. M. Janosi, T. Tel, D. E. Wolf, and J. A. C. Gallas, Phys. Rev. E. **56**, 2858 (1997).
[28] M. L. Ekiel-Jeżewska and E. Wajnryb, Phys. Rev. E **83**, 067301 (2011).
[29] M. L. Ekiel-Jeżewska, *CDROM Proceedings of the XXII International Congress of Theoretical and Applied Mechanics*, edited by J. Denier, M. D. Find, and T. Mattner (University of Adelaide, Adelaide, 2008).
[30] J. M. Nitsche and G. K. Batchelor, J. Fluid Mech. **340**, 161 (1997).
[31] A. Myłyk, W. Meile, G. Brenn, and M. L. Ekiel-Jeżewska, Phys. Fluids **23**, 063302 (2011).
[32] M. L. Ekiel-Jeżewska, Phys. Rev. E **90**, 043007 (2014).
[33] S. Jung, S. E. Spagnolie, K. Parikh, M. Shelley, and A. K. Tornberg, Phys. Rev. E **74**, 035302(R) (2006).
[34] S. Kim and S. J. Karrila, *Microhydrodynamics. Principles and Selected Applications* (Dover, New York, 2005).
[35] W. H. Press, S. A. Teukolsky, W. T. Vetterling, and B. P. Flannery, *Numerical Recipes in FORTRAN. The Art of Scientific Computing* (Cambridge University Press, Cambridge, 1992), pp. 727–731.
[36] See Supplemental Material at http://link.aps.org/supplemental/10.1103/PhysRevE.92.023026 for the movies and their description.
[37] M. Bukowicki, M. Gruca, and M. L. Ekiel-Jeżewska, J. Fluid Mech. **767**, 95 (2015).
[38] M. Müller, *Information Retrieval for Music and Motion* (Springer-Verlag, Berlin, 2007).
[39] M. Vlachos, G. Kollios, and D. Gunopulos, *Proceedings of 18th International Conference on Data Engineering* (IEEE, Piscataway, NJ, 2002), pp. 673–684, http://dx.doi.org/10.1109/ICDE.2002.994784.